JOC The Journal of Organic Chemistry

Article

pubs.acs.org/joc

Origin of Regioselectivity in α-Humulene Functionalization

Ulrich Neuenschwander, Barbara Czarniecki, and Ive Hermans*

Department of Chemistry and Applied Bio-Sciences, ETH Zurich, Wolfgang-Pauli-Str. 10, 8093 Zurich, Switzerland

Supporting Information

ABSTRACT: Humulene is a sesquiterpene with an important biochemical lead structure, consisting of an 11-membered ring, containing three nonconjugated C=C double bonds, two of them being triply substituted and one being doubly substituted. As observed by many groups, one of the two triply substituted C=C double bonds is significantly more reactive. In order to rationalize this peculiar regioselectivity, the conformational space of humulene has been explored computationally using various DFT functionals. Four different conformations were identified. Each conformation is chiral and has two enantiomeric forms, yielding a total of eight conformers. The potential energy surface for the interconversion of these conformers was characterized via intrinsic reaction coordinate analyses. Furthermore, an evaluation of the microcanonical partition functions allowed for a quantification of the entropy contributions and the calculation of the temperature dependent equilibrium composition. The results strongly suggest that the high regioselectivity is related to a strong, hyper-conjugative $\sigma_{C\alpha-C\beta}-\pi_{C=C}$ orbital overlap in the predominant conformations that discriminates one triply substituted double bond from the other. Furthermore, the order of magnitude of the calculated activation energies for the interconversions of the conformers is supported by NMR measurements at different temperatures.

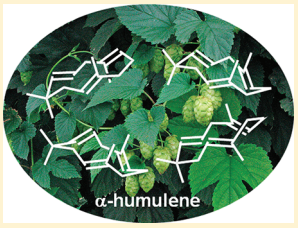

INTRODUCTION

α-Humulene ((1*E*,4*E*,8*E*)-2,6,6,9-tetramethylcycloundeca-1,4,8-triene or α-caryophyllene) is a naturally occurring monocyclic sesquiterpene consisting of three isoprene units. It is found in the essential oils of *Humulus lupulus* (Common Hop), from which its name is derived. Humulene and its oxidation products are responsible for the hoppy flavor of beer.

The epoxidation of humulene is a highly regioselective oxidative transformation.[1] In general, epoxidation of the C_1=C_2 bond (double bond i in Scheme 1) is favored over epoxidation of C_8=C_9 (double bond iii). For instance, using perbenzoic acid, less than 5% of **2** is obtained, along with more than 95% of **1**.[1a] The reason(s) for this peculiar behavior is not immediately evident. Note that the epoxidation of C_4=C_5 (double bond ii) is negligible because of the lower olefin number of C-substituents.

Scheme 1. Structure of Humulene (Three Distinct Double Bonds, Denoted as i, ii, and iii) and Its Regioselective Epoxidation

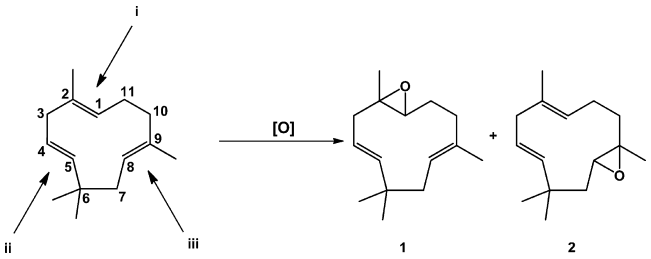

In earlier work, Shirahama et al. used force-field methods to characterize the conformations of humulene,[2] concluding that this medium-sized ring has three low-lying and one high-lying conformations. All of them are chiral, leading to a total of eight possible conformers. The experimental regioselectivity was rationalized through Mock's idea[3] that small torsional distortions of the double bond could determine the selectivity.

In this contribution, we aim for a full structural analysis of humulene using modern DFT calculations and temperature-dependent NMR studies in order to better understand the peculiar regioselective functionalization of this important medium-side ring.

RESULTS AND DISCUSSION

Identifying the Basic Conformations. Four different energy minima were identified on the potential energy surface, denoted below as A, B, C, and D. These minima correspond to four different conformations of humulene (see top of Scheme 2 and the Supporting Information). The most stable conformation A has a structure with the >C=C< fragments oriented "down−up−up"; i.e., the double bonds i, ii, and iii are pointing downward, upward, and upward, respectively, when going through the ring structure counterclockwise, starting at C1 (see Scheme 2). The second lowest conformation B is "up−up−up". The second highest conformation C is "up−down−up", and the highest conformation D is "up−up−down". Conformations A, C, and D are accessible from B via internal rotation around the C−C bonds (see Figure 1).

Since none of the conformations A−D feature an internal rotation−reflection axis (S_n with $n \in \mathbb{N}_0$), all of them are chiral; we define the enantiomers of A, B, C, and D in an arbitrary way as A*, B*, C*, and D*, respectively (Scheme 2). The double-bond orientation with respect to the ring-plane of a given

Received: January 12, 2012
Published: February 14, 2012

 © 2012 American Chemical Society dx.doi.org/10.1021/jo3000942 | *J. Org. Chem.* 2012, 77, 2865−2869

Scheme 2. Lewis Structures of the Different Humulene Conformers (A–D) and Their Enantiomers (A*–D*)

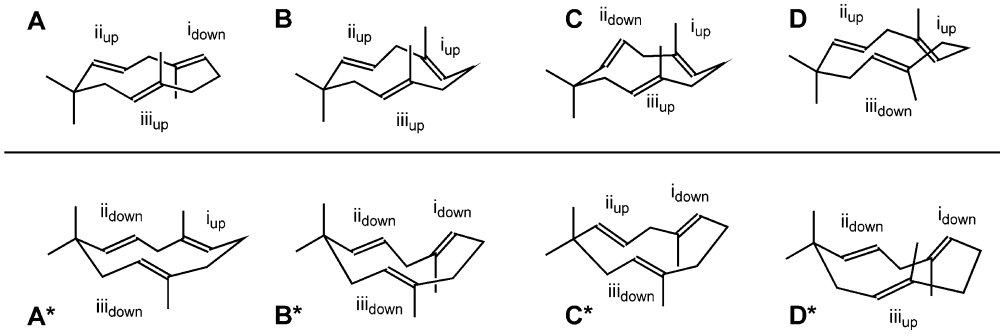

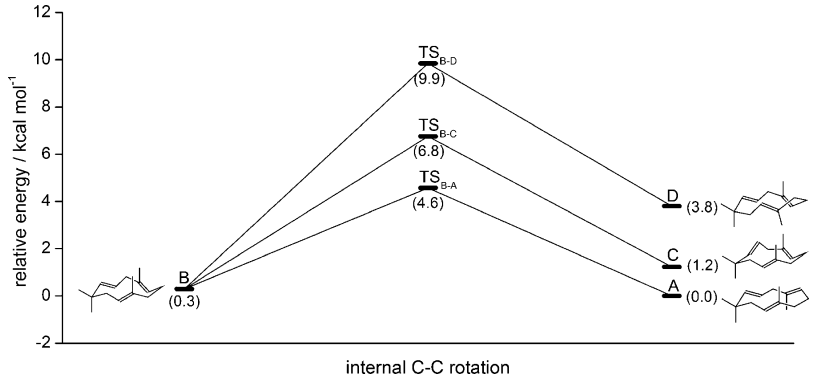

Figure 1. Conversion of conformer B into conformers A, C, and D; relative energies in kcal mol^{-1} (B3LYP/6-311++G(df,pd)//B3LYP/6-31G(d,p) level of theory).

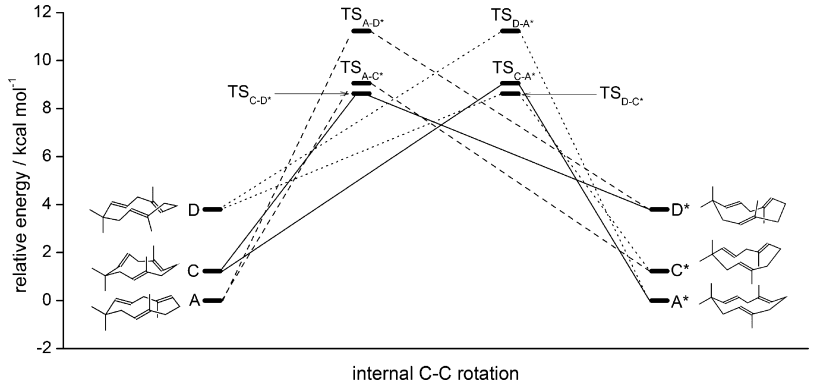

Figure 2. Conversion of conformers A, C, and D into conformers A*, C*, and D*; relative energies in kcal mol^{-1} (B3LYP/6-311++G(df,pd)//B3LYP/6-31G(d,p) level of theory).

enantiomeric conformer is inversed compared to its counterpart. For instance, conformer A is "down–up–up", whereas A* is "up–down–down" (see Scheme 2).

The interconversion of the four basic conformations occurs via internal C–C rotations, starting from the central conformation B, connecting to A, C, and D (Figure 1). The conformers A, C, and D can be converted into A*, C*, and D* as shown in Figure 2. A*, C*, and D* connect again with B*, similar to their enantiomers in Figure 1.

Shirahama et al. proposed that the conformational changes can be visualized in a cube,[2] with each corner nesting a conformation and the diagonals being the (imaginary) direct racemizations (Figure 3). Our results confirm these findings.

The ZPE-corrected relative energies of the four conformations, as well as the transition states (TSs) connecting them, are given in Table 1. Note that the B3LYP/6-311++G(df,pd)//

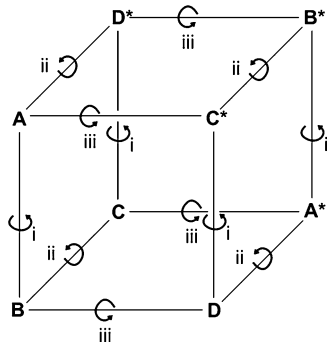

Figure 3. Full conformational space of humulene. Stars denote enantiomers (see Scheme 2).

dx.doi.org/10.1021/jo3000942 | J. Org. Chem. 2012, 77, 2865–2869

Table 1. Relative Energies of the Four Identified Humulene Conformations and Transition States, As Well As Their Partition Functions and Population Contributions at 298 K

conformer	ref[a] (kcal mol^{-1})	B3LYP[b] (kcal mol^{-1})	B3LYP-D[c] (kcal mol^{-1})	CAM-B3LYP[d] (kcal mol^{-1})	wB97[e] (kcal mol^{-1})	Q_{tot}[a] (m^{-3})	pop[f] (%)
A–A*	0.0	0.0	0.0	0.0	0.0	8.74×10^{44}	42.9
B–B*	0.2	0.3	0.2	0.3	0.3	1.37×10^{45}	45.6
C–C*	1.1	1.2	0.9	1.3	1.2	1.36×10^{45}	11.4
D–D*	3.6	3.8	4.05	4.0	4.2	1.36×10^{45}	0.15
TS(B → A)	10.6	4.6	5.7	5.0	6.3	2.73×10^{44}	
TS(B → C)	12.1	6.8	6.6	7.0	7.3	3.36×10^{44}	
TS(B → D)	14.4	9.9	10.0	10.4	11.25	2.56×10^{44}	
TS(A → C*)	16.9	9.1	9.2	9.5	10.0	4.28×10^{44}	
TS(A → D*)	13.8	11.2	11.6	11.9	13.05	2.61×10^{44}	
TS(C → D*)	13.5	8.6	9.75	9.1	9.8	2.21×10^{44}	

[a]Force field calculations by Shirahama et al.[2] [b]B3LYP/6-311++G(df,pd)//B3LYP/6-31G(d,p) level of theory.[6] [c]B3LYP/6-311++G(df,pd)//B3LYP/6-31G(d,p) level of theory including Grimme's dispersion corrections at single point level.[5] [d]CAM-B3LYP/6-311++G(df,pd)//CAM-B3LYP/6-31G(d,p) level of theory.[7] [e]wB97/6-311++G(df,pd)//wB97/6-31G(d,p) level of theory.[8] [f]At 298 K, on the basis of average stability of the conformers at B3LYP-D, CAM-B3LYP, and wB97 level of theory and the B3LYP-based partition functions.

B3LYP/6-31G(d,p) level has recently been benchmarked against the G2M method for the conformational analysis of cyclooctene.[4] Additionally, we verified that Grimme's dispersion corrections[5] barely affect the relative energies. The B3LYP[6] results were also found to be in good agreement with results obtained with the CAM-B3LYP[7] and wB97[8] functionals, which take into account long-range interactions. The agreement with Shirahama's force field calculations is remarkably good for the stable conformations.[2] However, a systematic overestimation of the transition state energies by about 5 kcal mol^{-1} can be observed with respect to modern DFT calculations.

In order to calculate the equilibrium population of the conformations, the partition functions Q_{tot} were evaluated according to eq 1. Q_{trans} refers to the translational partition function (three-dimensional particle-in-a-box model), Q_{rot} is the rotational partition function (rigid rotor model), and Q_{vib} is the vibrational partition function (harmonic oscillator model).[9] The equilibrium constants for the isomerization between two arbitrary conformations i and j can be computed using van't Hoff eq 2.

$$Q_{tot} = Q_{trans} \times Q_{rot} \times Q_{vib} \quad (1)$$

$$K_{i \to j} = \frac{[j]}{[i]} = \frac{Q_j}{Q_i} \times \exp\left(-\frac{E_j - E_i}{RT}\right) \quad (2)$$

According to these calculations, conformations A and B contribute nearly equally to the population, i.e., 42.9 and 45.6%, respectively, at room temperature (see Table 1). The temperature dependence of the equilibrium composition is plotted in Figure 4. The results suggest that conformation B is slightly more populated than the ground-state conformation A because of entropic effects.

It is interesting to note that McPhail et al. reported the X-ray structure of the A* conformer in a bis-$AgNO_3$ form;[10] the obtained geometric parameters are in very good agreement with our predictions.

NMR experiments (0.3 M humulene in CD_2Cl_2, ^1H 700 MHz, ^{13}C 176 MHz, 173–310 K) were carried out in order to verify and substantiate the proposed conformational rearrangements (assignment of the ^1H and ^{13}C chemical shifts were done on the basis of $^1H^{13}C$ HMQC, $^1H^{13}C$ HMBC, and $^1H^1H$ COSY experiments; see the Supporting Information). For

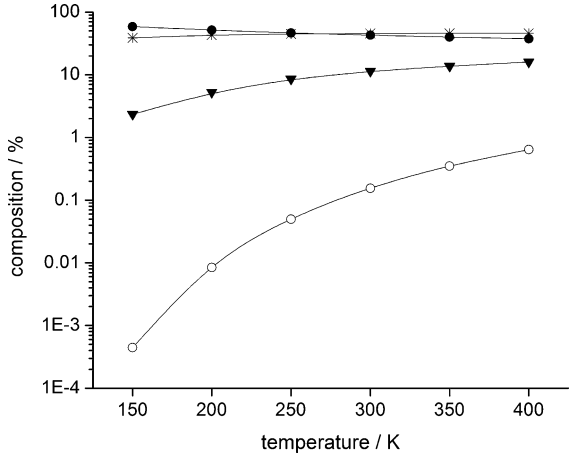

Figure 4. Equilibrium composition at different temperatures. Conformations A–A* (●), B–B* (*), C–C* (▼) and D–D* (○).

instance, in ^{13}C NMR, the *gem*-methyl groups appear as a broad singlet at 26.8 ppm at 303 K, reach coalescence at 273 K, and appear as two sharp singlets at 23.2 and 30.3 ppm at 213 K (see Figure 5). This coalescence behavior was simulated and found to be described by an activation energy of 10.5 ± 0.5 kcal mol^{-1}, which is in good agreement with the value reported in the literature, i.e., 10.6 ± 0.3 kcal mol^{-1}.[11] Note that for a coverage of the complete conformational space, i.e., all eight conformers, the two reactions with the highest barriers, i.e., B → D (*idem* for B* → D*) and A → D* (*idem* for A* → D), are actually obsolete. The highest remaining barrier, i.e., 9.1–10.0 kcal mol^{-1} for A → C* (see Table 1), is in excellent agreement with the experimental barrier of 10.5 ± 0.5 kcal mol^{-1}.

Moreover, from 193 K on downward, the appearing sharp singlet at 23.2 ppm begins to broaden as well. A similar behavior could be observed for the signals of C2, C3, and C7 (see the Supporting Information). Even though scanning the full coalescence range and performing robust spectra simulation cannot be accomplished in the technically achievable temperature range, these secondary processes suggest conformational changes with much lower activation energies, i.e., < 10 kcal mol^{-1}. This observation corroborates the validity of the DFT-predicted low activation energy values as given in Table 1.

Origin of Regioselectivity. It is generally accepted that epoxidation occurs, as many other electrophilic reactions, at the

dx.doi.org/10.1021/jo3000942 | J. Org. Chem. 2012, 77, 2865–2869

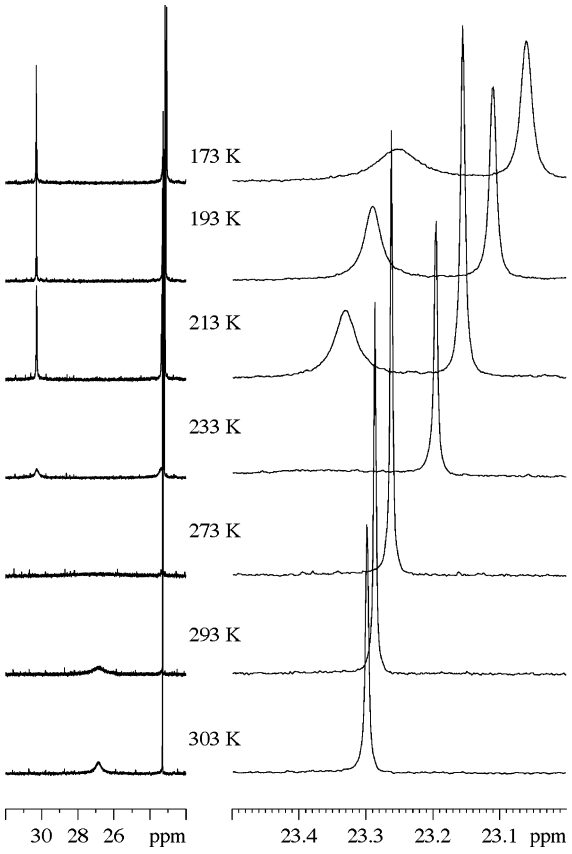

Figure 5. Temperature-dependent ^{13}C NMR spectra (176 MHz, CD_2Cl_2) of the *gem*-dimethyl group (more spectra are available in the Supporting Information).

double bond with highest electron density. By means of hyperconjugation of the allylic σ_{C-C} orbitals, the electron density can be increased substantially. Such hyperconjugation can only occur when the allylic σ_{C-C} orbital is perpendicular to the olefin's plane. It is interesting therefore to look at the dihedral angles (θ) in the most populated A and B conformations of humulene (Figure 6). In fact, for the

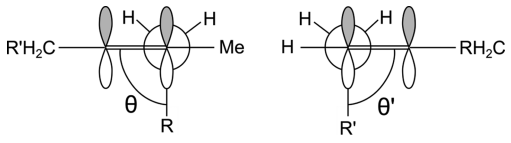

Figure 6. Newman projection of the triply substituted double bond fragment.

conformation A, the values of θ and θ' are 89 and 81° for the i double bond but 106 and 127° for the iii double bond. Moreover, for the conformation B, the values of θ and θ' are 98° (the hyperconjugation of σ_{C-H} dominates) and 130° for the i double bond but 106 and 112° for the iii double bond. As a consequence, orbital overlap is significantly better for the i double bond in the dominant conformations.

To exemplify the consequences for the region selectivity, we calculated the activation energies for the Prilezhaev epoxidation[12] (Table 2) and found the functionalization of the i double bond to be favored by approximately a factor of 6, in good agreement with the experimental observations. Note that by analysis of the stereochemical outcome of such a Prilezhaev

Table 2. Computed Barriers for the Prilezhaev Epoxidation with Peracetic Acid

conformer	double bond	E_b [a] (kcal mol^{-1})	relative reactivity[b]
A	i	9.9	6.2
A	iii	11.2	1

[a]B3LYP/6-311++G(df,pd)//B3LYP/6-31G(d,p) level of theory. [b]At 298 K and assuming identical activation entropies.

epoxidation, it could be ruled out experimentally that conformation B would contribute to the reaction flux.[1a] This is in agreement with our prediction showing an almost perfect θ-value for the i double bond in the A conformation.

In this context, it is important to mention the work of Haya and Hirose on the acid-catalyzed isomerization of humulene.[13] Also in this case, the double bond i was preferably protonated to deploy the cascade of reactions, further supporting the interpretation that the peculiar selectivity is mainly electronic, rather than steric as suggested earlier[14]

CONCLUSIONS

Four conformations of humulene, A, B, C, and D, have been characterized. Because of their chirality, four enantiomeric counterparts are possible. Racemization occurs via internal rotation around C−C bonds, and consequently, there are eight conformers in total. The high regioselective preference for the double bond i during epoxidations and acid-catalyzed isomerizations is rationalized by hyperconjugation between the allylic substituents and the π orbital increasing the double bond's electron density. The range of the calculated activation energies for the conformer interconversions is in agreement with variable temperature NMR experiments.

EXPERIMENTAL SECTION

All calculations were performed at the indicated level of theory with Gaussian 09.[15] The transition states connecting the different conformations were subjected to intrinsic reaction coordinate (IRC) analyses (the zero point of these IRCs was chosen arbitrarily).

^1H and ^{13}C NMR spectra were recorded on a 700 MHz spectrometer. The sample (humulene, Aldrich) was measured as 0.3 M solution in CD_2Cl_2 in nonspinning mode. ^1H and ^{13}C shifts are given in parts per million (ppm), referenced to external tetramethylsilane. The multiplicities of the signals are abbreviated as follows: s = singlet, d = doublet, t = triplet, br = broad, m = multiplet. For the assignment of the ^1H and ^{13}C chemical shifts, standard $^1H^{13}C$ HMQC, $^1H^{13}C$ HMBC, and $^1H^1H$ COSY experiments were measured using standard pulse sequences. Temperature calibration was performed using a sample of 4% MeOH in CD_3OD containing a trace of HCl.[16]

^1H NMR (700 MHz, CD_2Cl_2, 310 K): δ 5.65 (dt, J = 15.9 Hz, J = 7.5 Hz, 1H, C4*H*), 5.22 (dt, J = 5.9 Hz, J = 1 Hz, 1H, C5*H*), 5.02 (m, 1H, C1*H*), 4.94 (m, 1H, C8*H*), 2.55 (d, J = 7.4 Hz, 2H, C3H_2), 2.18−2.11 (m, 4H, C10H_2 and C11H_2), 1.97 (d, J = 7.34 Hz, 2H, C7H_2), 1.69 (s, 3H, C2−CH_3), 1.50 (s, 3H, C9−CH_3), 1.11 (s, 6H, C6−CH_3).

^{13}C NMR (176 MHz, CD_2Cl_2, 310 K): δ 140.9 (s, *C5*), 139.1 (s, *C2*), 133.0 (s, *C9*), 127.7 (s, *C4*), 125.8 (s, *C1*), 124.9 (s, *C8*), 41.9 (s, *C7*), 40.4 (s, *C3*), 39.7 (s, *C10*), 37.2 (s, *C6*), 26.8 (br s, C6−CH_3), 23.3 (s, *C11*), 17.6 (s, C2−CH_3), 14.8 (s, C9−CH_3).

^1H NMR (700 MHz, CD_2Cl_2, 203 K): δ 5.62−5.56 (m, 1H, C4*H*), 5.13 (d, J = 15.8 Hz, 1H, C5*H*), 4.94 (t, J = 7.7 Hz, 1H, C1*H*), 4.82 (d, J = 14.1 Hz, 1H, C8*H*), 2.53−2.48 (m, 1H, C3H_2), 2.45−2.41 (m, 1H, C3H_2), 2.16−2.11 (m, 1H, C10H_2), 2.11−2.04 (m, 3H, C11H_2 and C7H_2), 1.96−1.89 (m, 1H, C10H_2), 1.67 (d, J = 14.4 Hz, 1H, C7H_2), 1.60 (s, 3H, C2−CH_3), 1.41 (s, 3H, C9−CH_3), 1.04 (s, 3H, C6−CH_3), 1.02 (s, 3H, C6−CH_3).

dx.doi.org/10.1021/jo3000942 | J. Org. Chem. 2012, 77, 2865−2869

^{13}C NMR (176 MHz, CD_2Cl_2, 203 K): δ 141.0 (s, *C5*), 139.9 (s, *C2*), 133.2 (s, *C9*), 127.6 (s, *C4*), 124.8 (s, *C1*), 124.8 (s, *C8*), 41.3 (s, *C7*), 40.5 (s, *C3*), 39.6 (s, *C10*), 37.6 (s, *C6*), 30.3 (s, C6−CH_3), 23.3 (s, C6−CH_3), 23.1 (s, *C11*), 17.8 (s, C2−CH_3), 15.1 (s, C9−CH_3).

■ ASSOCIATED CONTENT

Supporting Information

Cartesian coordinates of the optimized conformations and transition states, as well as 1D and 2D NMR spectra at variable temperature. This material is available free of charge via the Internet at http://pubs.acs.org.

■ AUTHOR INFORMATION

Corresponding Author

*E-mail: hermans@chem.ethz.ch.

Notes

The authors declare no competing financial interest.

■ ACKNOWLEDGMENTS

The authors acknowledge the financial support from the Swiss National Science Foundation (SNF) and ETH Zurich.

■ REFERENCES

(1) See, e.g., (a) Damodaran, N. P.; Dev, S. *Tetrahedron* **1968**, *24*, 4123. (b) Yang, X.; Deinzer, M. L. *J. Org. Chem.* **1992**, *57*, 4717.

(2) Shirahama, H.; Osawa, E.; Matsumoto, T. *J. Am. Chem. Soc.* **1980**, *102*, 3208.

(3) Mock, W. L. *Tetrahedron Lett.* **1972**, 475.

(4) Neuenschwander, U.; Hermans, I. *J. Org. Chem.* **2011**, *76*, 10236.

(5) (a) Grimme, S. *J. Comput. Chem.* **2004**, *25*, 1463. (b) Grimme, S. *J. Comput. Chem.* **2006**, *27*, 1787.

(6) (a) Becke, A. D. *J. Chem. Phys.* **1992**, *96*, 2115. (b) Becke, A. D. *J. Chem. Phys.* **1992**, *97*, 9173. (c) Becke, A. D. *J. Chem. Phys.* **1993**, *98*, 5648. (d) Lee, C.; Yang, W.; Parr, R. G. *Phys. Rev. B: Condens. Matter Mater. Phys.* **1988**, *37*, 785.

(7) Yanai, T.; Tew, D.; Handy, N. *Chem. Phys. Lett.* **2004**, *393*, 51.

(8) Chai, J.-D.; Head-Gordon, M. *J. Chem. Phys.* **2008**, *128*, 084106.

(9) (a) Steinfeld, J. I.; Francisco, J. S.; Hase, W. L. *Chemical Kinetics and Dynamics*; Prentice Hall: Upper Saddle River, NJ, 1989. (b) Eyring, H. *J. Chem. Phys.* **1934**, *3*, 107.

(10) Apparently, the A and A* conformers lead to enantiopure crystals; by coincidence, the A* form was characterized: (a) McPhail, A. T.; Sim, G. A. *J. Chem. Soc. B* **1966**, 112. (b) McPhail, A. T.; Reed, R. I.; Sim, G. A. *Chem. Ind.* **1964**, *23*, 976.

(11) Dev, S.; Anderson, J. E.; Cormier, V.; Damodaran, N. P.; Roberts, J. D. *J. Am. Chem. Soc.* **1968**, *90*, 1246.

(12) Sienel, G.; Rieth, R.; Rowbottom, K. T. In *Epoxides, Ullmann's Encyclopedia of Industrial Chemistry*;Wiley-VCH: Weinheim, Germany, 2000.

(13) Naya, Y.; Hirose, Y. *Chem. Lett.* **1973**, 727.

(14) See, e.g., (a) Sattar, A.; Forrester, J.; Moir, M.; Roberts, J. S.; Parker, W. *Tetrahedron Lett.* **1976**, *17*, 1403. (b) Baines, D.; Forrester, J.; Parker, W. *J. Chem. Soc., Perkin Trans.* **1974**, 1598. (c) Dauben, W. G.; Hubbell, J. P.; Vietmeyer, N. D. *J. Org. Chem.* **1975**, *40*, 479. (d) Allen, F. H.; Brown, E. D.; Rogers, D.; Sutherland, J. K. *Chem. Commun.* **1967**, 1116.

(15) Frisch, M. J.; Trucks, G. W.; Schlegel, H. B.; Scuseria, G. E.; Robb, M. A.; Cheeseman, J. R.; Scalmani, G.; Barone, V.; Mennucci, B.; Petersson, G. A.; Nakatsuji, H.; Caricato, M.; Li, X.; Hratchian, H. P.; Izmaylov, A. F.; Bloino, J.; Zheng, G.; Sonnenberg, J. L.; Hada, M.; Ehara, M.; Toyota, K.; Fukuda, R.; Hasegawa, J.; Ishida, M.; Nakajima, T.; Honda, Y.; Kitao, O.; Nakai, H.; Vreven, T.; Montgomery, J. A., Jr.; Peralta, J. E.; Ogliaro, F.; Bearpark, M.; Heyd, J. J.; Brothers, E.; Kudin, K. N.; Staroverov, V. N.; Kobayashi, R.; Normand, J.; Raghavachari, K.; Rendell, A.; Burant, J. C.; Iyengar, S. S.; Tomasi, J.; Cossi, M.; Rega, N.; Millam, N. J.; Klene, M.; Knox, J. E.; Cross, J. B.; Bakken, V.; Adamo, C.; Jaramillo, J.; Gomperts, R.; Stratmann, R. E.; Yazyev, O.; Austin, A. J.; Cammi, R.; Pomelli, C.; Ochterski, J. W.; Martin, R. L.; Morokuma, K.; Zakrzewski, V. G.; Voth, G. A.; Salvador, P.; Dannenberg, J. J.; Dapprich, S.; Daniels, A. D.; Farkas, Ö.; Foresman, J. B.; Ortiz, J. V.; Cioslowski, J.; Fox, D. J. *Gaussian 09*, Revision A.02; Gaussian, Inc.: Wallingford, CT, 2009.

(16) van Geet, A. L. *Anal. Chem.* **1970**, *42*, 679.